JTTEE5 16:524–532
DOI: 10.1007/s11666-007-9072-1
1059-9630/$19.00 © ASM International

Peer Reviewed

Improved Protection Properties by Using Nanostructured Ceramic Powders for HVOF Coatings

T. Varis, J. Knuuttila, E. Turunen, J. Leivo, J. Silvonen, and M. Oksa

(Submitted October 27, 2006; in revised form May 25, 2007)

The potential of the high-velocity oxy-fuel (HVOF) thermal spray process for reduced porosity in coatings compared to those produced by other ambient thermal spray processes is well known. The ability to produce high-density ceramic coatings offers potential in high-performance applications in the field of wear, corrosion resistance, and dielectric coatings. However, due to operational limit of the HVOF process to effectively melt the ceramic particles, the process—structure relationship must be well optimized. It has been also demonstrated that benefits from HVOF ceramic coatings can be obtained only if particles are melted enough and good lamella adhesion is produced. One strategy to improve melting of ceramic particles in relative low-flame temperatures of HVOF process is to modify particle crystal structure and composition. In this paper the effect of the powder manufacturing method and the composition on deposition efficiency of spray process as well as on the mechanical properties of the HVOF sprayed are studied. Effect of fuel gas, hydrogen vs. propane, was also demonstrated. Studied materials were alumina-, chromia-, and titania-based agglomerated powders. Coating properties such as microstructure, hardness, abrasive wear resistance, and relative fracture toughness were compared to the coating manufactured by using conventional fused and crushed powders. It can be concluded that powder size distribution and microstructure should be optimized to fulfill process requirements very carefully to produce coatings with high deposition efficiency, dense structure, improved fracture toughness, and adhesion.

Keywords fatigue and fracture, HVOF microstructures, nanocrystalline composites, nano-powders, production/preparation technology, testing

1. Introduction

Oxide ceramics has been employed many years in applications were high abrasive wear resistance is needed together with special high-temperature properties like high oxidation resistance and chemical stability.

Traditionally coatings are applied by plasma spraying, which gives enough melting for materials with high melting temperature. Recently, it has been reported that it is possible to manufacture very dense ceramic coatings with high wear resistance with high-velocity oxy-fuel (HVOF) process, which is basically designed for metal and cermets spraying. It has been demonstrated that wear resistance of HVOF-sprayed ceramic coatings can be five to ten times better compared to plasma-sprayed ceramics (Ref 1-4). Advantageous for HVOF process is the high velocity of exhaust gases producing high velocity for spray particles, which were fed radially onto the combustion chamber. However, the critical factor, which is limiting the use of HVOF process for ceramics, is the melting capacity of relatively low-temperature flame. It has been shown that benefits from HVOF can be obtained only if particles are melted enough to have good lamella adhesion (Ref 3, 5). Limitation of process temperature emerges usually in low deposition efficiency (DE) and therefore DE demonstrates very well the melting capacity of the process. It is also generally known that critical factor in applicability of HVOF process for ceramics is the low DE, which currently limits the use of most HVOF processes for the economical way to produce ceramic coatings (Ref 6, 7).

Many studies have recently focused on nanostructured materials and their performance as thermally sprayed coatings. It has been shown that by introducing agglomerated nanostructured ceramic powder, fracture toughness of the coating can be improved (Ref 8, 9). Some role for improved performance is explained to have with unmelted nanosized material remaining inside the agglomerate. Some authors have reported these ''nanopockets'' to improve crack propagation resistance also for HVOF-sprayed ceramic coating (Ref 8, 9). Fracture toughness or cracking resistance of thermally sprayed coating is not easy to demonstrate. The fracture toughness of thermally sprayed coating cannot be defined as a pure material property. Lamella cohesion and portion of contact area of lamellas are strongly influencing on the mechanical properties of the coating (Ref 8, 10).

T. Varis, E. Turunen, and **M. Oksa**, VTT Technical Research Center of Finland, P.O. Box 1000, Metallimiehenkuja 8, Espoo, 02044 VTT, Finland; and **J. Knuuttila**, **J. Leivo**, and **J. Silvonen**, Millidyne Oy, Tampere, Finland. Contact e-mail: tommi.varis@vtt.fi.

In agglomeration process nano-micron sized powders are mixed together with binder and suspension is spray dried in chamber to form powder; spray drying is followed by sintering. Via agglomeration and sintering route the powder shape is spherical and porous. Fused and crushed powders are irregular and angular shape, but initial structure is fully dense. It is represented that special characteristic of agglomerated powders is their ability to form mixture phases more easily during spraying than fused and crushed powder blends. This is attributed to the closely mixing of constituents and relatively high surface area between small-sized particles (Ref 9, 11, 12).

In this study the effect of the powder morphology, density, and composition on mechanical properties and cracking behavior of the coating are considered. TiO_2-, Al_2O_3- and Cr_2O_3-based powders produced by agglomerated and sintered (a/s) and fused and crushed (f/c) production method were compared. High importance is put also on the role of melting capacity of the process on the resulted coating microstructure and mechanical performance.

2. Experimental Procedure

2.1 Materials

Used spray powders were TiO_2-, Al_2O_3- and Cr_2O_3-based pure ceramic or ceramic composite powders.

Agglomerated and sintered experimental nanostructured powders were manufactured by Millidyne Oy, having compositions presented in the Table 1. Fused and crushed TiO_2 (Amperit 782.8), Al_2O_3-13% TiO_2 (Amdry 6224), and Cr_2O_3-25%TiO_2 powders were manufactured by H.C. Starck, Sulzer Metco and Norton, respectively.

Powders were characterized by measuring particle size distribution by using Beckman Coulter LS 13320 analyzer and by studying powder morphology by using Philips XL30 scanning electron microscope.

2.2 Thermal Spray Test Setup

Powders were mainly sprayed by using Praxair HV 2000 HVOF spray gun, which was equipped with 22 mm chamber nozzle giving highest melting capacity. Used burning gases were hydrogen and propane. Titania powders, as an exception, were sprayed with 19 mm chamber to avoid nozzle clogging. In HV 2000 system powder is fed radially onto combustion chamber where powder starts to melt. Due to relatively low melting point (1840 °C) and small fraction of TiO_2, it melts too effectively in the chamber and causes clogging onto barrel throat. TiO_2 powder was not therefore possible to spray with 22 mm chamber. For comparison the TiO_2 was also sprayed by DJ Hybrid HVOF spray gun equipped with longer hydrogen nozzle (Air Cap type: DJ-3603). Spray parameters used for spray tests were selected to produce highest particle temperature. Parameter selection was based on the work carried out previously at VTT and is presented detailed elsewhere (Ref 4).

The feeding of small-sized ceramic powders with tight fraction required for HVOF spraying is often problematic. Thermico CPF-2HP powder feeder, which is specially designed for small powder particle feeding was therefore used.

Coatings were sprayed over carbon steel test plates having sizes of 25 mm × 50 mm × 2 mm and 40 mm × 50 mm × 2 mm to be used for microstructural characterization, hardness, and cracking studies as well as for rubber wheel abrasion tests. The test plates were mounted on 127 mm diameter cylinder for DE test, which were carried out mainly according to ISO/DIS 17836:2002-standard. Cylinder and plates were grit blasted in prior to coating with blocky corundum particles, size of 590-710 μm. During the coating spray gun was moved up and down continuously on the rotating cylinder. Altogether 120 gun passes were made continuously and DE was determined between the passes 21 and 120. To get an accurate value for powder feed rate, the powder was weighed before and after the actual spray. The weight of the resulting coating was determined.

2.3 Coating Characterization

Coating characterization was carried out by using JEOL JSM-6400 scanning electron microscope (SEM) and analyzed with an energy dispersive X-ray analyser (EDX). The crystal structures of some of the coatings were

Table 1 Used powders and measured particle size distributions

Material composition	Powder type	Primary particle size, μm	Measured particle size, μm		
TiO_2, Neoxid 1028-25, Millidyne	a/s	TiO_2 d50: 0.083 (63.3% <0.1 μm)	d10: 7.7	d50: 14.5	d90: 22.5
TiO_2, Amperit 782.8, H.C. Starck	f/c		d10: 6.2	d50: 11.7	d90: 20.0
Al_2O_3-13TiO_2, Neoxid 1042-32, Millidyne	a/s	Al_2O_3 d50: 0.370 (2.72% <0.1 μm) TiO_2 d50: 0.083 (63.3% <0.1 μm)	d10: 8.1	d50: 17.1	d90: 30.5
Al_2O_3-13TiO_2, Neoxid 1042-25, Millidyne	a/s	Al_2O_3 d50: 0.370 (2.72% <0.1 μm) TiO_2 d50: 0.083 (63.3% <0.1 μm)	d10: 7.2	d50: 13.9	d90: 22.6
Al_2O_3-13TiO_2, Amdry 6224, Sulzer Metco	f/c		d10: 7.8	d50: 15.8	d90: 26.9
Cr_2O_3-25TiO_2, Neoxid 1044-25, Millidyne	a/s	Cr_2O_3 d50: 0.370 (2.72% <0.1 μm) TiO_2 d50: 0.083 (63.3% <0.1 μm)	d10: 7.1	d50: 13.9	d90: 23.1
Cr_2O_3, 3031, Norton	f/c	Cr_2O_3 d50: 0.370 (2.72% <0.1 μm) TiO_2 d50: 0.083 (63.3% <0.1 μm)	D10: 7.5	d50: 14.6	d90: 24.1

characterized by x-ray diffraction by using Philips PW 3710 with Mo-K-alfa radiation. Rubber-wheel abrasion tests were carried out according to standard ASTM G 65D. Round-shaped quartz particles, which have an average size of 250 μm, were used as an abrasive. The wear distance was 2140 m. Rubber-wheel abrasion test is earlier demonstrated to give additional feedback from lamella adhesion along with material wear performance itself (Ref 3).

Hardness of the coatings was determined by Vickers microhardness method using a mass of 300 g.

The cracking behavior of the manufactured coatings was investigated by indenting the coating cross-section with Vickers tip at a 5 kg load. Marks were performed at the center of the cross-section and one diagonal was parallel to substrate. The crack lengths resulted from indentation were measured. Based on the indentation load (P) and crack length ($2c$), the crack propagation resistance was calculated according to the relation $P/c^{3/2}$ where P is in Newton and c in meter (Ref 13).

3. Results and Discussion

3.1 Powders

Powder compositions, measured particle sizes, and powder types are presented in Table 1. Typical very smooth surface morphology of agglomerated TiO_2 powder consisting nanosized primary particles is presented in Fig. 1(a). Initial structure of powder cross section in more detailed can be seen from surface of fracture in Fig. 1(b). Powder morphology and geometry is presented in Fig. 2(a-f). Typical spherical geometry of agglomerated spray-dried powder with some ''donut'' shaped geometry can be observed in Fig. 2(a-c). Typical blocky powder geometry of fused and crushed powders is seen on Fig. 2(d-f). The difference between particle shapes makes the volumetric size distribution comparison between agglomerated and crushed more complex.

However, in acceptable limits, the size distributions of the powders are very well comparable.

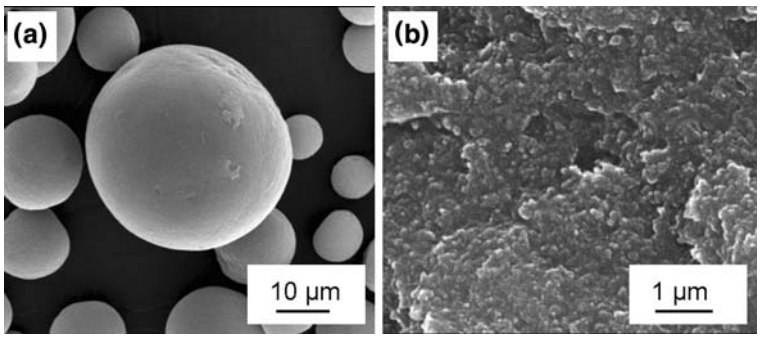

Fig. 1 (a) SEM picture from the TiO_2 powder particle surface, where smooth particle surface typical for agglomerate manufactured from very fine primary particle. (b) Cross section of TiO_2 powder particle

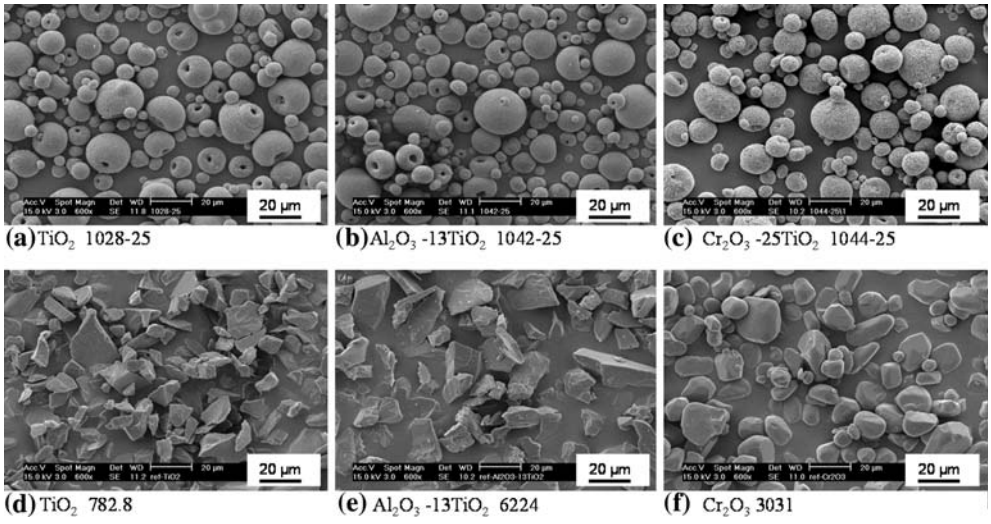

Fig. 2 SEM pictures from the powder particle surface showing the morphology and geometry of the powder

3.2 Coating Microstructure and Phase Structure

Microstructures for the coatings manufactured by using propane as fuel gas are presented in Fig. 3(a-l). X-ray diffraction curves for a/s and f/c Al_2O_3-13%TiO_2-coatings are presented in Fig. 4. In some of the coatings there are cracks in the top, which are formed during specimen preparation when epoxy resin is penetrated into the coating and contracted during hardening. In general, the overview on coating microstructures shows that very dense coating structures are produced.

Calculated porosity values with Leica Qwin V3 image analysis for the coatings shows higher porosity for a/s

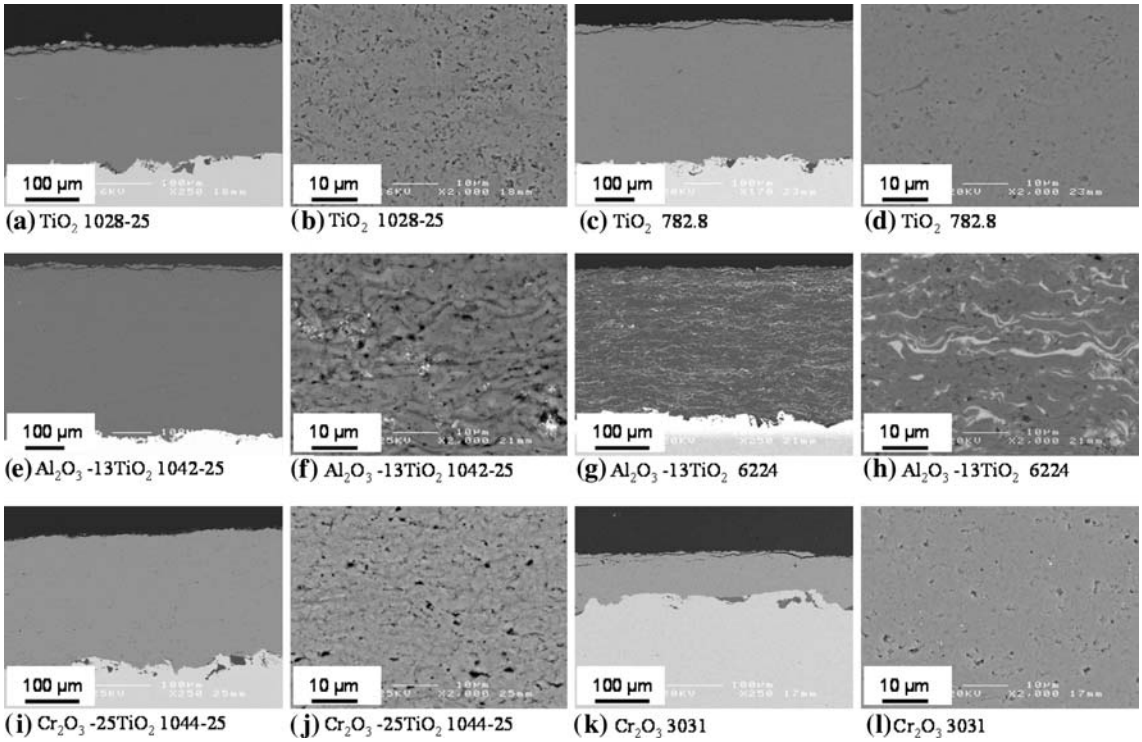

Fig. 3 Back scattered electron (SEM) images from the cross section of the coatings manufactured with propane as a fuel gas

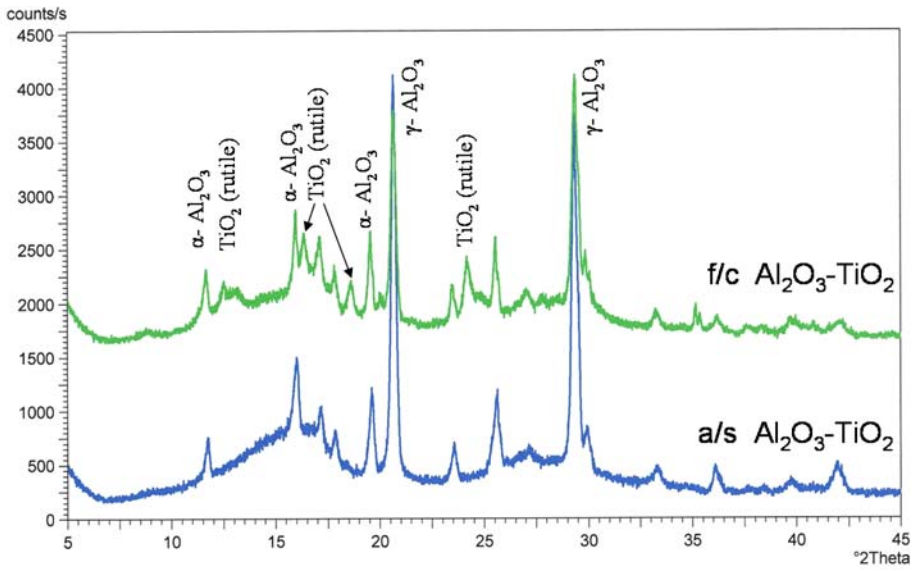

Fig. 4 X-ray patterns for Al_2O_3-TiO_2 coatings. From lower curve presenting the coating from a/s powder can be seen the missing rutile peaks

powder compared to f/c powder. The porosity for TiO_2, Al_2O_3-TiO_2, and Cr_2O_3-TiO_2 a/s powders were 2.81, 3.38, and 3.78%, respectively, whereas for f/c reference powders values were 0.74, 0.81, and 1.88%. There was clear difference in porosity between coatings manufactured with a/s and f/c powders. Higher porosity of coatings from a/s powder seems to be related with the original structure of the powder.

From the coating microstructures in Fig. 3(b) and (d) for titania relatively low lamella flattening for both TiO_2 coatings is observed and typical splat morphology with lamellar structure can actually not be clearly observed.

This is an indication of low melting stage of powder particles. By visual examination, it can be seen that one feature also for TiO_2 coatings seems to be relatively small lamella size compared to powder size distribution.

This means that biggest particles have bounced off from the substrate. Powder flattening ratio together with relatively small lamella size is showing that powder melting is not yet comfortable due to the spray nozzle used.

This is well correlated to DE measurements, which are presented below.

Al_2O_3-13%TiO_2 coatings are melted efficiently and clear lamellar structure can be observed. Comparison of the different Al_2O_3-TiO_2 coatings in Fig. 3(f) and (h) shows a clear difference in coating microstructures. TiO_2 shows as lighter areas in back scattered electron image. The coating made of f/c Al_2O_3-13%TiO_2 powder consists separate areas of Al_2O_3- and TiO_2-phases. In the coating made of a/s Al_2O_3-13%TiO_2 powder, the separate TiO_2 areas cannot be detected. In x-ray diffraction curves, which are presented in Fig. 4, there can be found some differences between coatings made from a/s and f/c. For an Al_2O_3-TiO_2 coating manufactured from f/c powder clear diffraction peaks from TiO_2 were no longer apparent, but for a coating manufactured from a/s powder no TiO_2 (rutile) peaks can be detected. With EDS chemical analysis it was confirmed that titanium is still present in the coating. From the x-ray curves it can be seen that the most of the powders original α-Al_2O_3 in both coatings was composed to metastable γ-Al_2O_3 during the rapid solidification process. In both coatings there is some α-Al_2O_3 remaining as a result of unmelted powder regions in the coating. Main difference is dissolution of nanosized TiO_2 into Al_2O_3 during spraying and formation of mixed phases during cooling, similarly than described Goberman et al. (Ref 12) for plasma-sprayed Al_2O_3-13%TiO_2. Phases formed cannot actually be detected from XRD-pattern, but probably these mixed phases occur as an amorphous state concluded from broad diffraction bands of a/s-powder in Fig. 4. That seems to occur only if TiO_2 is present as a nanosized in a/s powder not as micron sized in bulky f/c powder. This is the indication of formation of greater extent of mixed phases between Al_2O_3 and TiO_2 in the coating manufactured from a/s powder compared to coating manufactured from f/c powder. Similar results have also been reported by Normand et al. for plasma-sprayed Al_2O_3-TiO_2 coatings (Ref 11).

In pure Cr_2O_3 coatings, having high melting temperature (>2330 °C), the lamella flattening is not clearly seen but in Cr_2O_3-25%TiO_2 coating the flattening degree of lamellas is clearly higher (Fig. 3i-l). This is associated mainly on effect of lower melting temperature achieved by TiO_2 adding. Lamella size of both Cr_2O_3-based coatings is relatively small compared to powder fraction, which is similar to the behavior of TiO_2 coatings. Also for Cr_2O_3 coatings this is well correlated to the low DE values presented later in this study.

Coating microstructure studies showed clearly that there are some areas where powder particles are not thoroughly melted. Some evidence of unmelted agglomerates in the coating structure was found. In coatings manufactured from a/s powders there proved to be more porosity remaining in the coating compared to coatings manufactured from f/c powders.

3.3 Deposition Efficiency

The results from DE tests are presented in Fig. 5. In general, the importance of optimal particle size distribution for the HVOF-process is clearly seen on results. Deposition efficiencies were very high for Al_2O_3-based materials. TiO_2 powders did not reach the same level because different spray nozzle was used to avoid clogging.

The used 19 mm chamber does not give same melting capacity as the 22 mm chamber. Clear correlation was obtained for coating microstructures and deposition efficiencies. To be able to increase the DE for TiO_2, the size distribution of powder should perhaps meet the requirement of 22 mm chamber. With DJ Hybrid the melting capacity was lower, but dense TiO_2 coating was still, however, possible to produce.

For Cr_2O_3 materials having higher melting point the DE values were relatively low and a clear need to reduce size distribution of powder to achieve sufficient melting was demonstrated. Composition with 25% TiO_2, however, gave some improvements on DE.

Comparison of results for hydrogen and propane showed clearly, with used parameters, that higher DE values are achieved with propane. The result is well understandable by considering the difference between particle velocities measured for propylene and hydrogen (Ref 3). Behavior of propane, in terms of velocity, is assumed to be rather similar to propylene. The higher particle velocity of hydrogen results in shorter dwell times and therefore produces lower DE.

The effect of different powder geometry is contradictory. A superior DE value was obtained for agglomerated Al_2O_3-TiO_2 powder compared to f/c Amdry 6224 powder having similar size distribution. However, for TiO_2 material DE values were rather similar when different powder structures with similar size distribution were used.

For Cr_2O_3-based powders the difference in DE between powders is rather due to difference in composition. It seems that with optimal size distribution there is no much difference in DE between agglomerated and crushed powders, even though agglomerated powder particle is relatively dense. However, crushed powder seems to be more critical for larger particles, which are not able to melt enough during spraying. This kind of advantageous

behavior of agglomerated powder is seen clearly while comparing the Amdry 6224 and Millidyne 1042-32 powders. Another possible explanation of higher DE for agglomerated powder is the ability of the powder to form low melting mixed phases between Al_2O_3 and TiO_2 or Cr_2O_3 and TiO_2 more easily than crushed ones like discussed earlier.

When comparing the porosity of TiO_2 a/s-powder and f/c-powder, higher porosity for a/s-powder can be noticed. The higher porosity of a/s-powder is thought to be originating from the initial structure of a/s powder particle which is not thoroughly melted or lower ability of a/s-powder to deform and fill the irregularities of the surface. However, for both powders DE was at the same level, which shows that agglomerated powder form can be deposited as effectively as crushed powders even if the porosity of coating becomes higher. Therefore it seems that a/s-powder may not be able to elastically rebound from substrate so easily, but form coating even if the melted portion of the particle is lower.

3.4 Wear Resistance and Hardness

The volume loss of coatings in rubber wheel test is presented in Fig. 6 and hardness of coating is presented in Fig. 7. In general it is seen that the wear performance of Cr_2O_3-based coatings compared to the alumina- or titania-based coatings was superior.

Main interest was to demonstrate the difference between different manufacturing routes on the wear

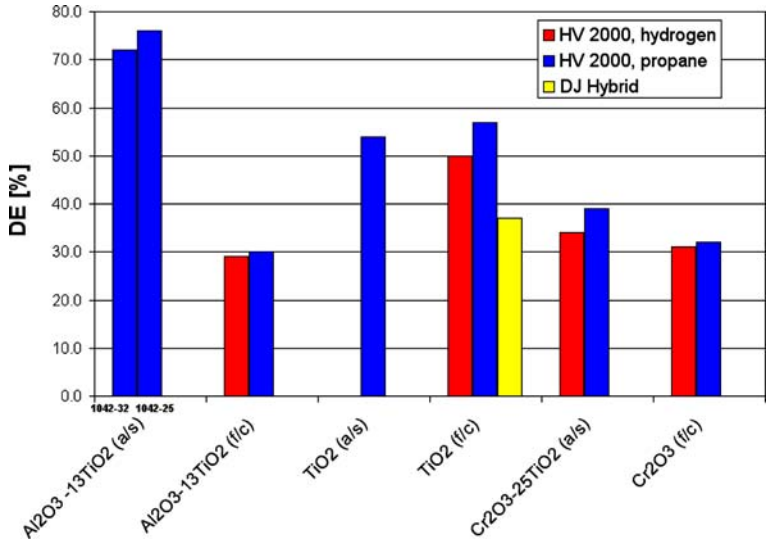

Fig. 5 Deposition efficiency results for tested powders

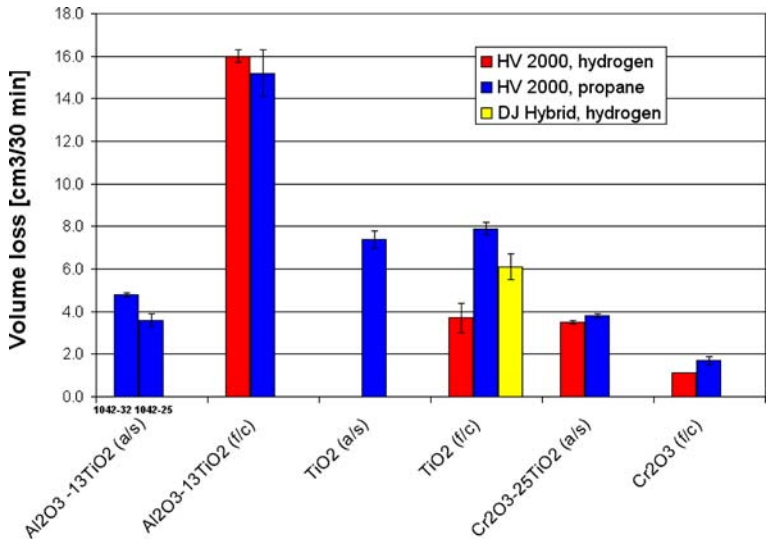

Fig. 6 Wear resistance of manufactured coatings

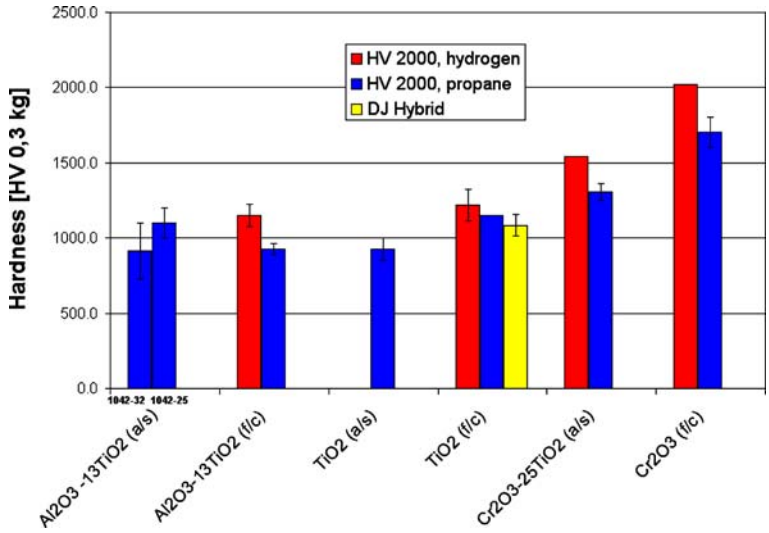

Fig. 7 Vickers hardness of the coatings with 0.3 kg load

performance of the coating. The difference in wear performance for pure TiO_2 coating was not significant. However, for Al_2O_3-TiO_2 coating the significant difference in wear performance can be demonstrated. Poorer wear performance of the coating made of f/c (blend) powder may be related with difference in phase structure between a/s and f/c powder. In the coating manufactured from f/c powder, the size and distribution of TiO_2 phases are different from coating made of a/s powder as seen on Fig. 3(f) and (h). Larger TiO_2 phase areas, as a softer phase, are more prone to wear than Al_2O_3 with used abrasive particles in wear test. In coating manufactured from a/s powder separate TiO_2 areas are missing and titanium is presenting as Al_2O_3-TiO_2 phases. However, higher wear rate of coating manufactured from f/c-powder cannot only be linked on softer phase effect because wear rate of Al_2O_3-TiO_2 coating is higher than TiO_2 coatings. There are problems in Al_2O_3 cohesion as well, which causes increased wear due to lamella peel off.

Notable result was also the better wear performance of coating made of a/s TiO_2 powder compared to the coating made of f/c powder. Higher porosity at a/s coating structure did not weaken the wear performance of coating. Wear resistance of the coatings in this type of test is shown earlier to be strongly influenced by lamella cohesion (Ref 4), which probably shows to be advantageous for agglomerated nanopowders. This mechanism is linked to easier melting of nanosized particles on the surface of agglomerated particle.

Obtained hardness values seem not to explain or demonstrate the coating quality detailed enough. Poor wear performance in wear test of the coating produced from f/c Amdry 6224 powder could not be predicted from hardness value, but wear test indicates weak lamella cohesion very clearly. On the other hand for TiO_2, the better hardness values measured for coating manufactured from f/c powder did not give any advantage in wear test.

The hardness values are influenced on the porosity inside the lamella, which is not hindering the wear performance.

It can be observed that DE values achieved did not correlate with the performance in wear test. This result indicates that low DE does not correlate with weak lamella contact. It rather seems that those particles which were attached to the surface forming a coating, were all then well adhered. This appears for Cr_2O_3 coatings sprayed with HV 2000 and TiO_2 coating sprayed with DJ Hybrid, which shows similar behavior having good wear resistance despite the very low DE measured for the process.

Better DE values were achieved by using propane than by using hydrogen, which is most likely connected to the higher melting degree in propane spraying. However, while comparing propane and hydrogen as a fuel gas, the wear resistance of coatings sprayed with hydrogen was 10-100% better than coatings sprayed with propane. Al_2O_3-TiO_2 manufactured from f/c powder is an exception. It seems that important factor for high wear resistance seems to be related to particle velocity, which is reported to be higher when using hydrogen (Ref 3). Higher wear resistance in hydrogen spraying could therefore be explained with better interlamellar contact. For both gases the parameters for HV 2000 were already selected to produce highest particle temperature and velocity at that condition is fixed and dependent on the fuel gas used.

3.5 Cracking Behavior Under Vickers Tip

Crack propagation resistance for some selected coatings sprayed by propane as a fuel gas is presented in Fig. 8. Main result from the cracking study was minor cracking of the coating manufactured from a/s Al_2O_3-TiO_2 powder. With SEM studies it is possible to observe significantly different cracking behavior between a/s and f/c Al_2O_3-13%TiO_2 coating. In coating manufactured from a/s the cracks were shorter and growing nicely from edge of indentation mark.

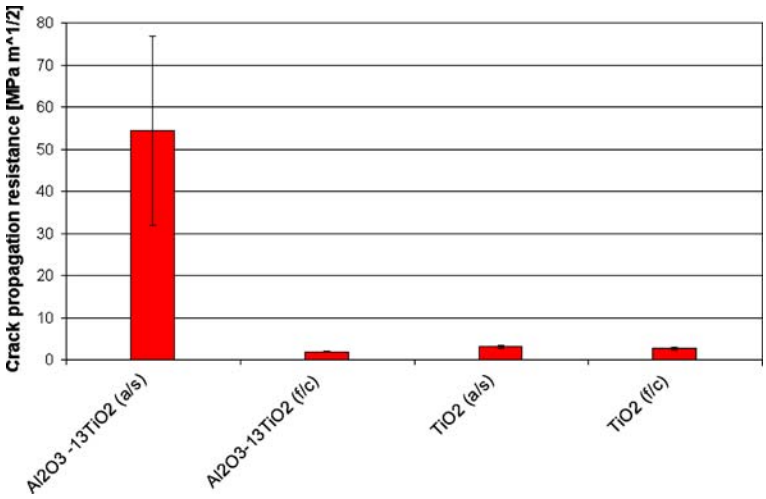

Fig. 8 Crack propagation resistance for coating sprayed with propane

In coating manufactured from f/c powder there were many longer cracks parallel to substrate plane.

Agglomerated nanocomposite Al_2O_3-TiO_2 coating with dense lamella structure seems to prevent cracking under Vickers load very effectively. The role of formation of mixed phases between alumina and titania as well as special pore structure in the lamella might have important influence on crack propagation resistance. TiO_2 coatings behaved rather similarly and there was not significant difference in cracking behavior between a/s and f/c coatings. Crack propagation resistance of the coating manufactured from a/s seems to be as low as for coating manufactured from f/c TiO_2 powder and any advantage on cracking resistivity could not be found by using nanosized agglomerated powder.

It can be considered that attribution of high crack propagation resistance is rather a result of high melting stage with good lamella adhesion than porous coating structure with weak lamella adhesion. This means that, in case of ceramic HVOF spraying, to achieve good coating properties the particle melting during spray process should be maximized. Clear evidence from the influence of so-called ''nanopockets'' on cracking tendency could not be found and it is believed that good cracking resistivity of Al_2O_3-TiO_2 coating is more effected by compositional changes than nanopocket effect. It can be concluded that the crack propagation resistance is influenced by pore structure, lamella adhesion, and material composition. According to these studies the significance of these factors cannot be separated, but it seems that by using agglomerated nanocomposite powders, good combination of different factors is possible to obtain, which is significantly lowering the cracking tendency of the coating.

4. Conclusions

In this paper the effect of powder geometry and composition on deposition efficiency, microstructure, and coating properties like wear resistance and cracking behavior of HVOF thermal spray ceramic coatings was studied. The present study has demonstrated some advantages that could be achieved by using agglomerated nanostructured powders.

The most significant characteristic found for agglomerated nanosized powders was the ability to form mixed phases more easily during spraying compared to crushed powders. In this study superior wear properties and fracture toughness were obtained for a/s Al_2O_3-13%TiO_2 coatings compared to coating manufactured from fused and crushed powder. Al_2O_3-TiO_2 coating manufactured from agglomerated and sintered powder showed very low cracking under Vickers tip compared to the coating manufactured from fused and crushed powder, which could be explained with phase structure along with the combination of good lamella bonding and special pore structure.

Key factor for DE was found to be particle size distribution along with material composition. Deposition efficiency values achieved were very high for Al_2O_3-based material, but TiO_2 and Cr_2O_3 did not fulfill the process requirements due to the nonoptimal particle size distribution for HVOF process. It was demonstrated that DE value does not directly correlate on coating performance on wear test. Some low DE coatings performed very well in wear test. It was found that DE can be increased by alloying agglomerated powder with nanosized second phase constituent, which is able to dissolve during spraying.

References

1. A.J. Sturgeon, M.F.D. Harvey, and F.J. Blunt, The Influence of Fuel Gas on the Microstructure and Wear Performance of Alumina Coatings Produced by the High Velocity Oxyfuel (HVOF) Thermal Spray Process, *Br. Ceramic Proc.*, 1997, **54**, p 5764
2. A. Kulkarni, J. Gutleber, S. Sampath, A. Goland, W.B. Lindquist, H. Herman, A.J. Allen, and B. Dowd, Studies of the Microstructure and Properties of Dense Ceramic Coatings Produced by Highvelocity Oxygenfuel Combustion Spraying, *Mater. Sci. Eng.*, 2004, **A369**(12), p 124-127

3. E. Turunen, T. Varis, S.P. Hannula, A. Kulkarni, J. Gutleber, A. Vaidya, S. Sampath, and H. Herman, On the Role of Particle State and Deposition Procedure on Mechanical, Tribological and Dielectric Response of High Velocity OxyFuel Sprayed Alumina Coatings, *Mater. Sci. Eng.*, 2006, **A415**(12), p 1-11
4. E. Turunen, T. Varis, T.E. Gustafsson, J. Keskinen, T. Fält, and S.P. Hannula, Parameter Optimization of HVOF Sprayed Nanostructured Alumina and Alumina–Nickel Composite Coatings, *Surf. Coat. Technol.*, 2006, **200**(1617), p 4987-4994
5. G. Bolelli, V. Cannillo, L. Lusvarghi, E. Turunen, T. Varis, T. Fält, and S.-P. Hannula, Wear Behaviour of APS and HVOF Sprayed Ceramic Coatings, *Building of 100 years of Success*, B.R. Marple, Ed., Proceedings of the 2006 International Thermal Spray Conference, May 15-18, Seattle Washington, USA, 2006, 7 p
6. Y. Shimizu, K. Sugiura, K. Sakaki, and A. Devashanapathi, An Attempt to Improve the Deposition Efficiency of Al_2O_3 Coating by HVOF Spraying, *Thermal Spray: Surface Engineering via Applied Research*, C.C. Berndt, Ed., May 8-11, International Thermal Spray Conference, Montreal, 2000, p 181-186
7. D.A.J. Ramm, T.W. Clyne, A.J. Sturgeon, and S. Dunkerton, Correlations between Spray Conditions and Microstructure for Alumina Coatings Produced by HVOF and VPS, *Thermal Spray Industrial Applications*, C.C. Berndt and S. Sampath, Ed., National Thermal Spray Conference, June 20-24, Boston, USA, 1994, p 239
8. R.S. Lima and B.R. Marple, From APS to HVOF Spraying of Conventional and Nanostructured Titania Feedstock Powders: A Study on the Enhancement of the Mechanical Properties, *Surf. Coat. Technol.*, 2006, **200**(11), p 3428-3437
9. H. Luo, D. Goberman, L. Shaw, and M. Gell, Indentation Fracture Behavior of Plasma Sprayed Nanostructured Al_2O_3–13 wt.%TiO_2 Coatings, *Mater. Sci. Eng.*, 2003, **A346**(12), p 237-245
10. R. McPherson and B.V. Shafer, Interlamellar Contact Within Plasma-Sprayed Coatings, *Thin Solid Films*, 1982, **97**(3), p 201-204
11. B. Normand, V. Fervel, and C. Coddet, Tribological Properties of Plasma Sprayed Alumina–Titania Coatings: Role and Control of the Microstructure, *Surf. Coat. Technol.*, 2000, **123**(12), p 278-287
12. D. Goberman, Y.H. Sohn, L. Shaw, E. Jordan, and M. Gell, Microstructure Development of Al_2O_3–13 wt.%TiO_2 Plasma Sprayed Coatings Derived From Nanocrystalline Powders, *Acta Mater.*, 2002, **50**(5), p 1141-1152
13. G.R. Anstis, P. Chantikul, B.R. Lawn, and D.B. Marshall, A Critical Evaluation of Indentation Techniques for Measuring Fracture Toughness. I. Direct Crack Measurements, *J. Am. Ceramic Soc.*, 1981, **64**(9), p 533-538